

Imaging Gene Expression: Detecting Gene Activation using Laser-induced Fluorecence

A project presented in partial fulfillment of the requirements
for the degree of Bachelor's of Science in Physics
from the College of William and Mary

by

Frank M. Wells

Advisor: Dr. William Cooke

Williamsburg, Virginia

May 2004

Abstract

This project we worked on developing a detector to image gene expression non-invasively. To image deeper than 60 microns into tissues, there is an 800-nanometer (650-900nm) window where the absorption of light by the tissue matter and by water is minimized. In this window skin tissue appears translucent, allowing for detection below the surface of the tissue (from outside the target) without the invasive techniques currently necessary. Using genes coded to produce fluorescent proteins near the 800nm window should make gene activation, the creation of amino acids and proteins, visible *in vivo*. This is difficult however, because the fluorescence is short lived and the scatter from the inducing laser is optically blinding compared to the fluorescence. Designing electronic circuits for driving the laser and gating an avalanching photodiode, to yield a short response time, ~ 1 ns, allows a detector to show that the fluorescence can be discriminated from scattered light when directed into a scattering medium (dye). We have shown the minimum dye concentration that still yields detectable light to be 1.75×10^{-6} molar corresponding to $\sim 2 \times 10^{13}$ molecules which is below the density of typical tissue samples.

Introduction

Genes contain the information used by cells to create amino acids, which organize into proteins that perform most major life functions. Current medical science is mapping the genome (complete set of genes) in hopes to understand both how genes create amino acids and what inter- or extra-cellular factors lead to the production of different types of amino acids. The method of observing these genes and their activation is called imaging gene expression. Detecting gene activation is very difficult and much of the data is collected through observing the products of the gene activity. Identifying individual genes allows medicine to treat an infection at its root rather than focusing on its results.

Current Methods

The two main methods to image gene expression include injecting radioactive substances into the subject and viewing the whole result. Methods that involve injecting interactive but non-harmful substances into tissue, and then observing their behavior, present an overall view of a sample, but they do not focus on any one specific gene. The problem with injecting such substances is that the body has natural processes to clean out foreign bodies and the substance tends to collect in the liver. The body's natural resistance presents materials that would otherwise not be located at the site of activating genes and thus interferes with the gene expression. The other spots where the injected substances collect merely show the location of certain genes rather than labeling their activation because the resulting image has insufficient resolution.

Non-injection techniques such as magnetic resonance imaging (MRI) and *in vivo* microscopy provide an incomplete picture of gene expression. The MRI can resolve images as small as a 10 μ m cube. Rather than targeting a specific gene it generates a picture of where gene activation is occurring. The closest MRIs have come to imaging genes has been monitoring transgene expression¹. Transgene expression is a special form of gene expression, it is observed when nano-particles or iron oxide are purposefully implanted into a sample so the resonant frequency of the surrounding area is shifted². It

principally reveals the delivery system or specific gene activation but the natural non-specific gene expression is the important information. *In vivo* microscopy focuses a laser on the sample and reads through the different layers of tissue. This method is very accurate but is only viable for shallow tissue samples (~ 60 μm).

These current methods of imaging gene expression are insufficient for viewing gene activation. While the MRI can locate gene activations and *in vivo* microscopy can identify individual genes, only invasive and surveying techniques can observe the results adequately. With a non-invasive solution, one could observe gene activation *in vivo* with no outside interference.

The 800nm Solution

In theory one can image deep tissue samples by exploiting the “800nm window”. There is an 800-nanometer (650-900nm) window where the absorption of light by both tissue matter and water are minimized. Hemoglobin in skin stops absorbing light around 650nm while water begins to absorb light at 900nm. In this window, skin tissue appears translucent, and subcutaneous skin is visible. Coupled with genes, modified to produce Infrared Fluorescing Proteins (IRFP), this provides means to distinguish an activating gene from its neighbors. After brief illumination from an 800nm laser the IRFP fluorescence from IRFP fluoresces. This induced fluorescence permeates out through the tissue. By filtering out light from scattering sources one may isolate the protein fluorescence and observe gene activation. Scattering off of large-scale impurities (known as Mie scattering) obscures the induced fluorescence; the purpose of this research is to distinguish the laser-induced fluorescence from the scattering interference.

Difficulties with Laser-Induced Fluorescence

This method presents a number of difficulties, the first of which is the timing to detect the fluorescence. The induced fluorescence is far less intense than the light provided by the laser. To ensure that the fluorescence is being detected, the remaining laser pulse must be negligible compared to the fluorescence; in essence, it must be off

before the detector turns on. The induced fluorescence, however, only lasts a few nanoseconds, so any photo-detector must activate after the laser is off and before the fluorescence dissipates to avoid being blinded by the laser. Secondly, despite having a high rise and fall time, the pulse still must reach a high enough intensity to induce detectable fluorescence in the tissue sample. Lastly, the fluorescence provided by the IRFP must be powerful enough to permeate to the surface of the tissue sample, so determining the maximum thickness of the tissue and minimum density of fluorescers allows detection of the underlying fluorescence.

Experiment Setup

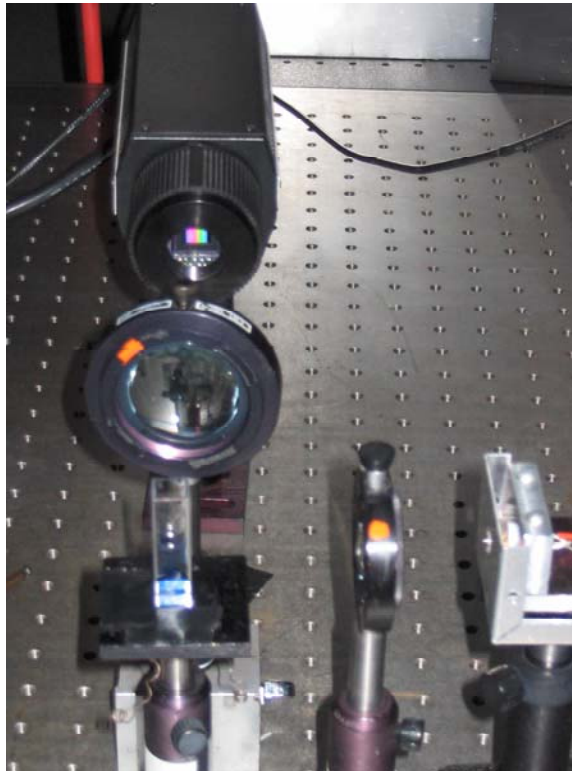


Figure 1 The laser setup. The laser is on the right, focused into a dye filled cuvette and a camera (used for aligning the APD) is placed orthogonal to the laser beam. The Avalanche Photodiode is on the left, out of the picture

The equipment used for this project includes:

- 850 nm Vertical Cavity Surface Emitting Laser (VCSEL) diode with a ball lens specifically a Lasermate VCT-A85A41-OH

- Avalanche Photo-Diode (APD)

- Function Generator
- Photo Meter
- Power Supply
- Electronic chips including NPN 7904 Transistors, 74123 Monostable

Univibrators, various resistors and capacitors

The VCSEL lases perpendicularly to the surface of the emitting film through a vertical, short cavity allowing for fast ($\sim 100\text{ps}$) rise and fall times for pulses and a high power output of $\sim 8\text{mW}^3$. The APD features increased signal gain compared to normal photodiodes and can detect at very fast time scales.

Methods

To distinguish the timing between the reflected laser light and the underlying fluorescence we developed a laser driver and detector circuit. Simply an emitter-follower, amplified the current from a function generator to drive the laser. This large current, 60mA, overloaded and burned the laser. We redesigned the laser driver circuit, Figure 2, using a Monostable Univibrator (one shot) which pulses once on an edge of an incoming signal and produces one peak which can vary in amplitude through the use of external capacitors and resistors. The output current is well within the tolerance of the VCSEL.

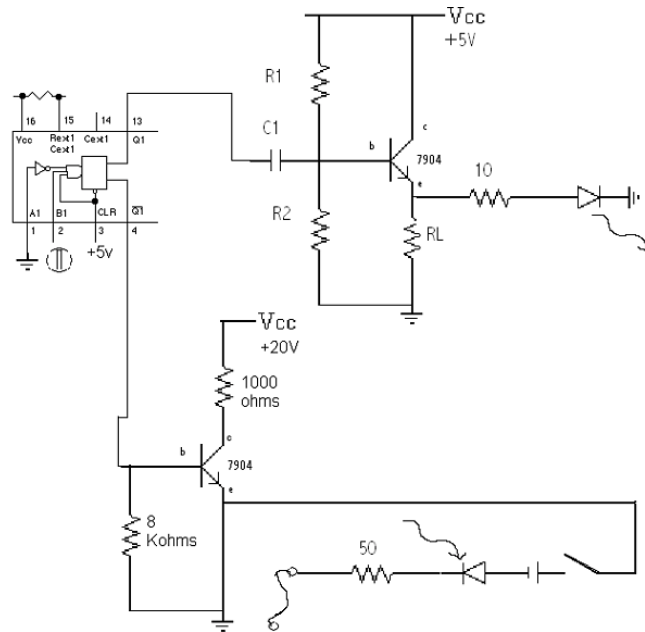


Figure 2 The circuit driven by Q from the one shot(top left) is the laser circuit and the circuit driven by Q_{bar} is the detector gating.

By using the same pulse from the univibrator the detector and the laser are synchronized so they can completely cool down and ensure minimal signal reflection and thermal lensing while still providing a fast pulse. The one shot leads into an AC coupled emitter follower to drive the laser. It sharpens the pulse by allowing the baseline of the driving pulse to hover around the turn-on voltage of the laser and increases the intensity by multiplying the current provided by the one shot. The circuit also drives a gating mechanism providing a back bias for a pin photo-detector so that it collects charge and has a shorter turn-on time.

We collimate the laser and focus it through a lens into a standard photo detector. Varying R_1 , R_2 , R_L and C_1 on the circuit diagram produces pulses as short as 1ns. Initially, we used a back biased pin diode photo-detector to characterize the laser and found that it can indeed operate at ~1ns. Since the laser responds at the fast time scale, we introduced the APD so that the induced signal can be detected despite its low intensity.

The APD amplifies the signal so that even dim fluorescence can be detected and distinguished from circuit noise. The difficulty lies in the properties of the avalanching gain. It is necessary to charge up the APD and detect only in the window of the induced fluorescence. Yet to ensure the APD will detect light there has to be light greater than the minimum threshold required for avalanching. This requires the use of a dye cell to characterize what time scale the fluorescence lasts and what density of fluorescing material the detector can image.

The IR 140 dye fluoresces at $\sim 800\text{nm}$ the wavelength of minimal absorption in tissue. Placing the APD orthogonal to the VCSEL path that is focused into the middle of a cuvette containing the dye mixture ensures that the fluorescence can be distinguished from laser scatter. We imaged the cuvette on a video camera to identify the induced fluorescence to separate it from laser scatter. The fluorescence permeates with the scattered light and creates two images, one due to the fluorescence from the dye and the other from scattering off the surfaces of the cuvette. With the detector properly aligned we measure the amount of fluorescence as a function of the dye concentration in the cuvette. With too little concentration, the light simply passes through the mixture with little interaction. However, if it is too dense, the light fluoresces and is reabsorbed before leaving the liquid. By varying the concentration, we can characterize the efficiency of the detector to distinguish fluorescence from scattered light.

Conclusions and Results

We can generate pulses ranging from 1ns to as long as 200ns. Thermal lensing limits the performance of the laser at high power and long pulse lengths. The lower end threshold provides information characterizing the rise and fall times of the laser. Using very fine changes to the driver circuit we were able to minimize the pulse width to $\sim 1\text{ns}$. Table 1 identifies the approach to the threshold resistance that no longer drives the laser.

R2 (Ω)	FWHM(ns)	peak power(mV)	PPxFWHM(nsxmV)
-----------------	----------	----------------	----------------

213.6	0	0	0
215.4	0.5	0.6	0.3
215.8	1.1	1.4	1.54
218.1	1.5	1.5	2.25
218.8	2	3	6
227.5	2.5	3.5	8.75
228	4	9	36
240	5	11.5	57.5
279	6	20	120
334	7	31	217
416	7.5	43	322.5
485	8.5	49	416.5
551	9	54	486
691	9.5	64	608
816	10	68	680
995	11	72	792

Table 1 The data table is under the conditions that $R_1=8.2\text{ K}\Omega$ and $R_L=1\text{ K}\Omega$

The data starts off very steep and then begins to flatten out. Figures 3 and 4 show the sharp cut off threshold of the laser in the FWHM and Peak Power vs. Resistance graphs.

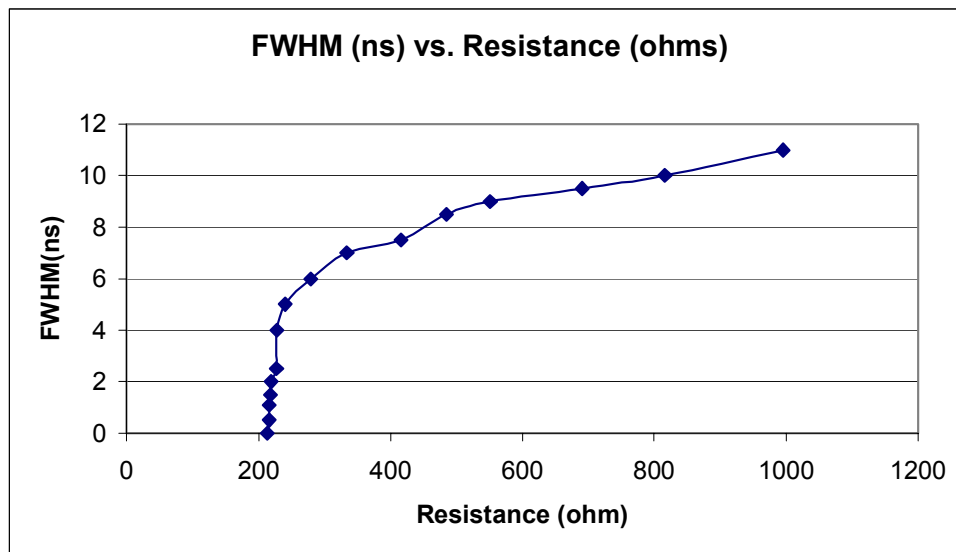


Figure 3

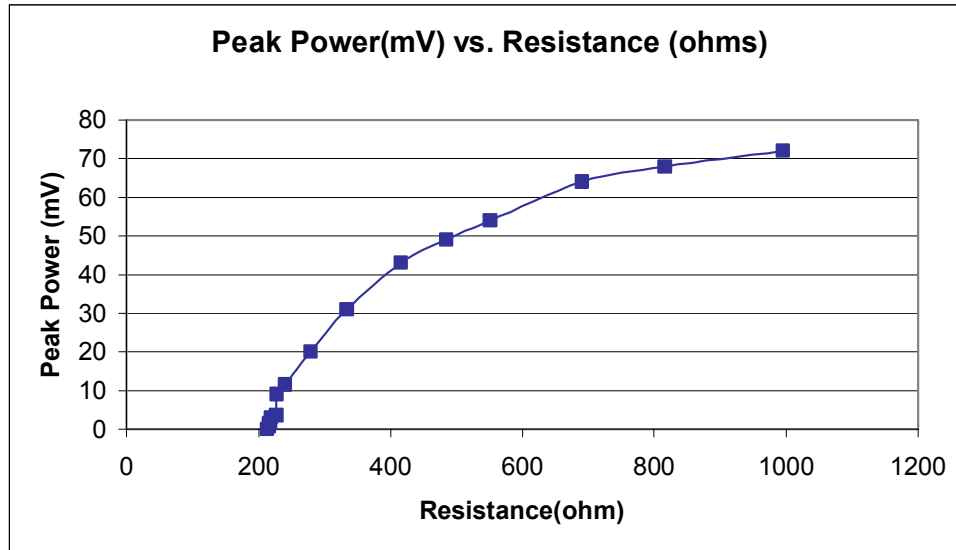


Figure 4

At 215.4 Ω the laser pulsed but at 213.6 Ω it did not. There was a very sharp cut off of the threshold resistance. The difficulty with running a laser at threshold with such sensitivity of $\sim 1 \Omega$ is that this may occur due to thermal effects in the electronics.

This demonstrated that the laser and detector have rise and fall times capable of operating at speeds of $\sim 1\text{ns}$. For the purposes of inducing the fluorescence the duration of the lasing is irrelevant, it matters how quickly it turns off and the detector turns on. Detectable 1ns pulses have turn-on and turn-off time of less than 1ns, and thus should be sufficient to allow detection of the resulting fluorescence. With a laser capable of testing the limits we needed for the detector, we moved on to characterizing the avalanching photodiode to see if it could meet the fast response requirements.

To test for saturation we drove the laser from 1hz to 1 MHz and discovered that the detected pulse signal is independent of the frequency. This implies that there are no thermal effects on the pulse size when driven by two very different frequencies. However, the laser varies with temperature while under a continuous wave condition, suggesting that each pulse is saturating the APD such that any decrease in signal due to thermal lensing is lost in too much power. To figure out this maximum photon threshold,

we first calculate the gain of the APD in Electrons/Photon. This is done through dimensional analysis of total power and total voltage of non-saturated measurement on the APD.

$$P = \left[\frac{J}{s} \right]$$

$$\frac{hc}{\lambda} = \left[\frac{J}{\text{photon}} \right]$$

$$f = \left[\frac{\text{pulse}}{s} \right]$$

$$\frac{P\lambda}{fhc} = \left[\frac{\text{photon}}{\text{pulse}} \right] \quad (1)$$

The same can be done to figure out the number of electrons per pulse, knowing that the pulse drops because it is terminated in 50Ω.

$$I = \frac{V}{R} = \left[\frac{C}{s} \right]$$

$$1.6 \times 10^{-19} = \left[\frac{C}{\text{electron}} \right]$$

$$\frac{I \times \text{pulsewidth}}{(1.6 \times 10^{-19})} = \left[\frac{\text{electron}}{\text{pulse}} \right] \quad (2)$$

Equation (2) divided by (1) yields the gain on the APD

$$\frac{Vhcf \times \text{pulsewidth}}{RP\lambda \times (1.6 \times 10^{-19})} = \left[\frac{\text{electron}}{\text{photon}} \right] \quad (3)$$

For a 65 ns pulse, total power of 27μW, with a 1000ns duty cycle using an 850 nm laser, a voltage drop of .5V over 50 Ω the gain was 33 $\frac{\text{electrons}}{\text{photon}}$. This is in

accordance with the factory shipped value of 30 $\frac{\text{electrons}}{\text{photon}}$ ⁴. The total number of

photons produced by one un-attenuated pulse is ~10¹⁰ photons. To do this, requires the attenuation of the signal such that there is a minimally recognizable pulse detected on the APD.

The threshold point was reached when we attenuated the laser with two neutral density filters, one ND 2.0 (1% transmission), the other ND 3.0 (0.1% transmission). The signal remained recognizable with both in place. However when a third was applied, ND .3(50% transmission), the signal became non-distinguishable from the noise. This means the minimum number of photons required to activate the APD to produce a signal distinguishable from the noise is $\sim 10^5$ photons, while still granting the gain. This value is very small compared to the laser-induced fluorescence so the detector is sufficient to image the fluorescence.

The next task is to determine whether or not the induced fluorescence can be distinguished from the scattered light. We simulate different tissue densities by varying concentrations of dye mixture, using LDS821, a purple colored dye that absorbs light around 800 nm and fluoresces around 570nm seemed ideal because of its absorption value. However, the detector is optimized for 800nm light and the fluorescence lay towards the lower threshold of detection. IR 140 dye, which both absorbs and fluoresces around the same wavelength of 800nm⁵ is a better choice because it more accurately represents conditions with the IRFP. Besides being more detectable, this dye is more practical because the fluorescence that is emitted by the tissue is should fluoresce at around the same wavelength it absorbs, ~ 850 nm. This ensures maximized detection potential for the APD.

I imaged the fluorescence onto the APD using an infrared camera to make sure the detector was at the spot of maximum intensity. The image it produces consisted of two parts, one bright spot and one horizontal dim line. The bright spots result from reflections off the entrance or exit walls of the cuvette. We move the position of the laser to maximize the horizontal beam and thus eliminate scattering off the cuvette, the optimal image is displayed in Figure 5. The horizontal line represents the fluorescence and so by placing the detector at the maximum intensity on the horizontal line the scattering interference is minimized.

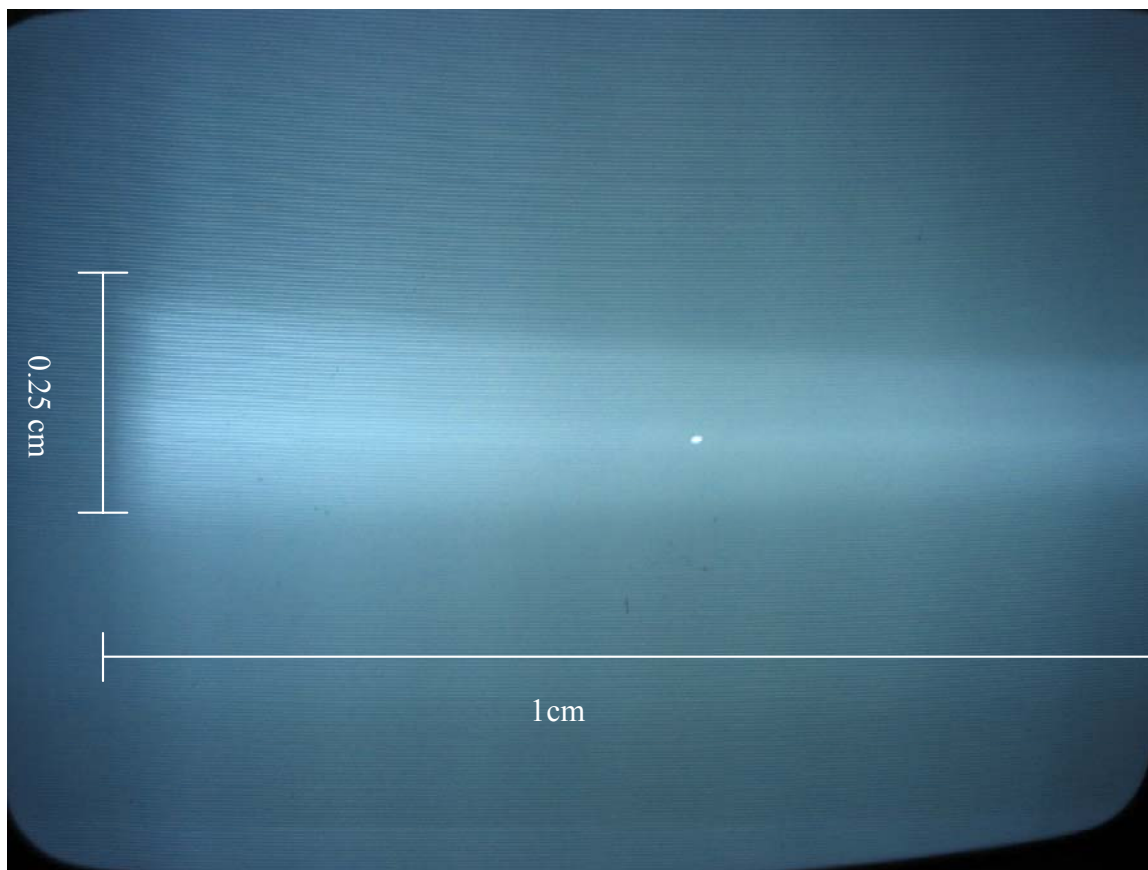


Figure 5 The laser beam enters the cuvette and is imaged onto the left hand side of the picture, notice the vertical wall where it begins at the edge of the glass. Notice it is brighter on the edge; it gets dimmer as it penetrates further into the medium. Dimensions of fluorescence is 1cm X 2.5mm

Then I varied the dye concentrations to see the effect on the amount of induced fluorescence, represented by Table 2.

Dye Concentration (molar)	Voltage(mV)
10^{-2}	0.66
0.5×10^{-2}	0.33
2.5×10^{-3}	1
1.25×10^{-3}	1.5
6.25×10^{-4}	1.75
3.13×10^{-4}	1.8
1.66×10^{-4}	1.8
8.31×10^{-5}	1.8
4.17×10^{-5}	1.8
2.8×10^{-5}	1.8
1.4×10^{-5}	1.75
7×10^{-6}	1.7
3.5×10^{-6}	1.5
1.75×10^{-6}	1.25
8.9×10^{-7}	1
Pure Methanol	1

Table 2 The dye concentrations are halved between the steps

The minimum amount of scatter expected would be from the methanol with dye concentration of zero. However, the dense concentrations (.0025 molar and above) actually fluoresce less than the minimum possible dye concentration as seen in Figure 6.

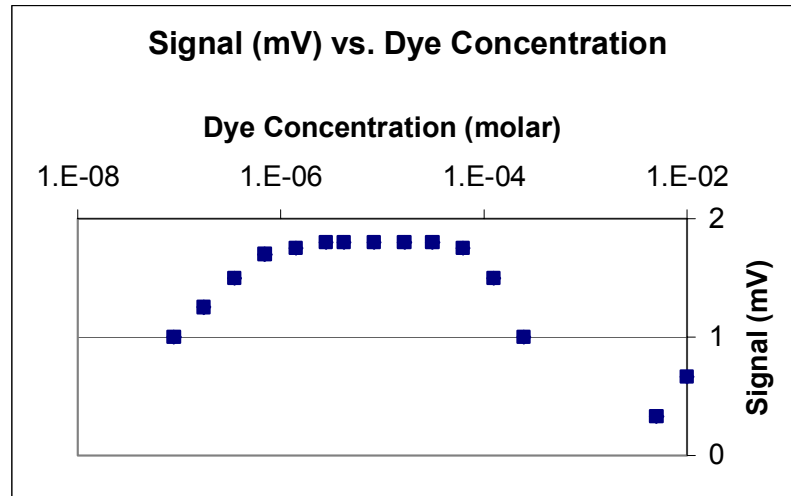


Figure 6 This plot is logarithmic on the x axis

This leads to the conclusion that the only induced fluorescence that is observed is the light that is detected on top above the intensity of the control value of pure methanol. The most efficient dye concentration is 4.2×10^{-2} molar because it is within the saturation peak so that despite minor fluctuation due to methanol evaporation it still provides the most amount of light from fluorescence. We placed it at the most intense spot of the initial fluorescence, which happened to be right where the laser enters the cuvette. The image on the camera became very faint confirming the re-absorption of the higher dye concentrations (when the highest concentration was placed in the cuvette).

The most interesting data in the present project comes from the minimum dye concentration. If the minimum number of dye molecules needed to have fluorescence is greater than the total amount of excitable molecules in DNA, then the detector can't image the activation of the genes because it would not be detectable. The size of the laser

beam and the width of the cuvette give the size of a fluorescing cylinder in the dye, and combined with the minimum dye concentration this yields the total number of molecules needed for fluorescence.

$$\begin{aligned}
 \text{volume} &= \pi R^2 L = [cm^3] \\
 [ml] &= [cm^3] \\
 \text{moles} &= \text{molar} \left[\frac{\text{moles}}{\text{liter}} \right] \times \pi R^2 L \\
 \text{molecules} &= 6.23 \times 10^{23} \left[\frac{\text{molecules}}{\text{mole}} \right] \times \text{moles}
 \end{aligned}$$

Using the dye concentration of 1.75×10^{-6} molar the total number of dye molecules is 2.07×10^{14} in the induced fluorescence volume in figure 5. This is taken for the whole volume of induced fluorescence however, the APD only images about a tenth of that because it is positioned at one edge and its area compared to the cross sectional area of the beam is small. Therefore only $\sim 2 \times 10^{13}$ molecules are needed to see fluorescence. This results in a density of $\sim 1 \times 10^{15} \frac{\text{molecules}}{cm^3}$. How does this compare to the number of molecules in DNA? In any one area there are $7.5 \times 10^6 = \frac{\text{nuclei}}{cm^2}$ (cells that have a nucleus with DNA)⁶. Assuming uniformity in size within a tissue sample, $1 \text{ cm}^3 = (7.5 \times 10^6)^{1.5} = 2 \times 10^{10} \frac{\text{nuclei}}{cm^3}$. With anywhere from $10^5 - 10^6 \frac{\text{gene}}{\text{nuclei}}$ ⁷ and between 1 and 1000 $\frac{\text{protein}}{\text{gene}}$ ⁸, the density of skin is above the minimum concentration (10^{15} to $10^{16} \frac{\text{gene}}{cm^3}$) to induce and detect fluorescence.

What is Next

Two main objectives lie ahead. First, gating the APD to operate with fast gain times to keep up with the short-lived fluorescence so that it will lower the blinding effect that the scattering in methanol versus the fluorescence rate with the dye. Second, characterizing and imaging tissue samples to determine maximum depth and fluorescence

intensity. Difficulties include most of the APD circuit cannot be easily tampered, with safely because it is soldered to the chipboard and covered with high voltage insulator.

¹ Schuster MD, Daniel P. "Picture This: Imaging Gene Expression in the Lungs," Gene Express, December 2003. <<http://www.thoracic.org/geneexpress/gene1203.asp>>

² Weissleder, Ralph et al. "In vivo magnetic resonance imaging of transgene expression." Nature Medicine. March 2000, 351-54.

³ Lasermate Group Inc. Single Mode VCSEL Diodes. Pomona, CA. 2003.

⁴ Hamamatsu Photonics K.K, Solid State Division. APD Module C5331 Series Instruction Manual. Tokyo: Hamamatsu Photonics K.K, Solid State Division. 8.

⁵ Exciton. Laser Dyes Catalog. Exciton. 1999

⁶ Hoath, Stephen B; Leahy D.G. "The Organization of Human Epidermis: Functional Epidermal Units and Phi Proportionality", J Invest Dermatol. 2003.121: 1440-1446. Abstract <<http://www.jidonline.org/cgi/content/abstract/121/6/1440>>

⁷ Dudroit, Sandrine; Gentleman, Robert. "Introduction to Genome Biology", Biconductor Short Course. Summer 2002. <<http://www.bioconductor.org/workshops/WyethCourse101702/GenBio/GenBio4.pdf>>

⁸ Professor Unknown. Biology 102 Lecture. University of Connecticut, Fall 2002. <http://www.sp.uconn.edu/~bi102vc/102f02/toedt/RNAproteinF2002web.htm>